

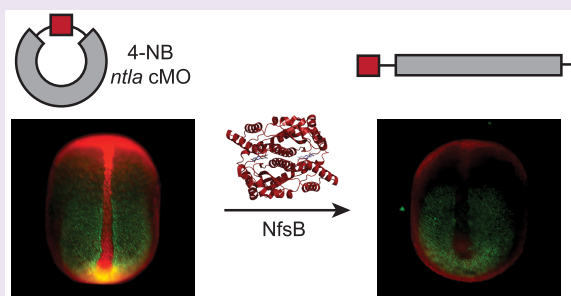
Nitroreductase-Activatable Morpholino Oligonucleotides for *in Vivo* Gene Silencing

Sayumi Yamazoe, Lindsey E. McQuade, and James K. Chen*

Departments of Chemical and Systems Biology and Developmental Biology, Stanford University School of Medicine, Stanford, California 94305 United States

S Supporting Information

ABSTRACT: Phosphorodiamidate morpholino oligonucleotides are widely used to interrogate gene function in whole organisms, and light-activatable derivatives can reveal spatial and temporal differences in gene activity. We describe here a new class of caged morpholino oligonucleotides that can be activated by the bacterial nitroreductase NfsB. We characterize the activation kinetics of these reagents *in vitro* and demonstrate their efficacy in zebrafish embryos that express NfsB either ubiquitously or in defined cell populations. In combination with transgenic organisms, such enzyme-actuated antisense tools will enable gene silencing in specific cell types, including tissues that are not amenable to optical targeting.



Non-natural oligonucleotides are valuable probes of biological systems, as they can convey synthetic control of endogenous nucleic acids with high sequence specificity.¹ In particular, morpholino oligonucleotides (MOs) have been used to block the expression of targeted genes in several invertebrate and vertebrate models.^{2–6} These nuclease-resistant polymers persist in live organisms for days and are typically designed to recognize 25-base sequences that span intron-exon junctions or translational start sites. The resulting blockade of RNA splicing or translation allows loss-of-function phenotypes to be determined within days, contrasting the months that can be required to obtain homozygous mutants. Thus, MOs are important counterparts to current mutagenesis and genome editing techniques.

The development of caged MOs (cMOs) has significantly extended the versatility of these reverse-genetic tools. Conventional MOs are typically used to constitutively disrupt targeted genes in an organism-wide manner. We and others have synthesized light-activatable cMOs that allow spatiotemporal control of RNA splicing or translation, complementing the use of conditional knockouts to study stage- and tissue-specific differences in gene function. Several MO caging strategies have been devised, employing hairpin structures,⁷ intermolecular duplexes,^{8,9} nucleobase modifications,¹⁰ or oligonucleotide cyclization.^{11,12} Light-dependent gene silencing can be achieved through whole-organism irradiation or the targeted illumination of specific cell populations. For example, we have applied light-activatable cMOs to interrogate transcription factor function during zebrafish notochord, pancreas, and vascular patterning.^{11,13,14}

Despite these advances, current cMO technologies lack the spatial control afforded by genetic methods. Tissues with complex three-dimensional morphology, significant depth, or rapid movement are challenging to selectively target by optical

techniques. We envisioned that enzyme-activatable cMOs could overcome these limitations, as the triggering enzymes could be expressed in individual cell populations using *cis* regulatory elements. We also anticipated that our cyclic cMO strategy could be adapted to accommodate enzyme-mediated activation. This approach involves the intramolecular cross-linking of 5' amine- and 3' disulfide-modified MO oligonucleotides using appropriately functionalized tethers, generating macrocyclic structures that conformationally resist RNA hybridization.¹¹ The 4,5-dimethoxy-2-nitrobenzyl (DMNB)-containing linkers used in our previous study allowed optical MO uncaging, but cyclic cMOs could accommodate enzyme-cleavable linkers as well.

To achieve enzyme-activatable cMOs, we focused on the *Escherichia coli* nitroreductase NfsB as the triggering catalyst. NfsB is a dimeric flavoprotein enzyme that has broad electron acceptor specificity¹⁵ and has been used in conjunction with prodrugs to selectively ablate cells in vertebrates.^{16,17} In particular, transgenic zebrafish lines that express *nfsB* in β cells, cardiomyocytes, or other cell types have been established, and their exposure to the metronidazole leads to the targeted loss of these cells.^{18,19} We surmised that cyclic cMOs containing an NfsB-cleavable linker could be used with analogous lines to knock down gene function in a tissue-specific manner (Figure 1a).

We first synthesized a bifunctional linker containing an NfsB-sensitive 4-nitrobenzyl (4-NB) group in 11 steps (Figure 1b). 4-Nitrobenzaldehyde (**1**) was reacted with allyltrimethylsilane in the presence of titanium(IV) chloride to give the homoallylic

Received: May 29, 2014

Accepted: July 22, 2014

Published: July 28, 2014

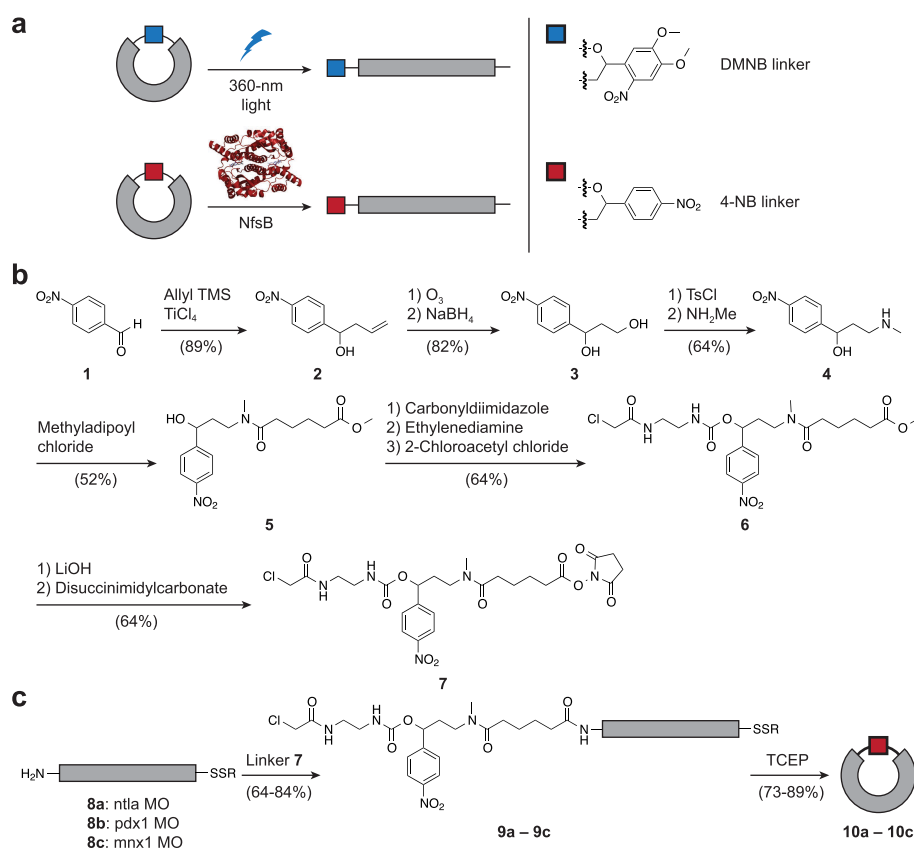


Figure 1. Design and synthesis of NfsB-activatable cMOs. (a) Schematic comparison of light-activatable DMNB cyclic cMOs and NfsB-activatable 4-NB cyclic cMOs. (b,c) Synthetic routes for the 4-NB bifunctional linker and 4-NB cyclic cMOs.

alcohol **2**. The terminal olefin of **2** was oxidatively cleaved and reduced to obtain 1,3-diol **3**, which was converted to the 1,3-aminoalcohol **4** through tosylation and treatment with methylamine. The secondary amine of **4** was condensed with methyladipoyl chloride to yield methyl ester **5**, and the secondary alcohol of **5** was sequentially conjugated with ethylenediamine and 2-chloroacetyl chloride to obtain chloroacetamide **6**. Methyl ester hydrolysis and *N*-hydroxysuccinimide coupling then provided the fully functionalized linker **7**. We next cyclized a 25-base MO targeting the mesodermal T-box transcription factor *no tail-a* (*ntla*), using previously described procedures (Figure 1c).¹¹ The 5' amine- and 3' disulfide-modified oligonucleotide (**8a**, 5'-GACTTGAGGCAGACATATTTCCGAT-3'; start codon underlined) was coupled with the linker in aqueous buffer to obtain the linear intermediate **9a**, and disulfide reduction with immobilized tris(carboxylethyl)phosphine (TCEP) yielded the 4-NB *ntla* cMO **10a** through intramolecular cyclization.

NfsB-catalyzed reduction of the 4-NB group in *ntla* cMO **10a** should generate a 4-hydroxylaminophenyl intermediate, which will rapidly undergo 1,6-elimination to cleave the carbamate linkage. The resulting methylenediene will then be quenched by water. To confirm that 4-NB cyclic cMOs can be linearized in this manner, we overexpressed mCherry-tagged NfsB in cultured mammalian cells and immunopurified the active enzyme with anti-mCherry serum. We then added the 4-NB *ntla* cMO to aqueous buffer containing NADH and varying amounts of NfsB-mCherry, achieving a final cMO concentration (2 μM) approximating that typically used for *in vivo* studies.⁴ The reaction was incubated at the standard temperature for zebrafish aquaculture (28.5 °C) and then analyzed by

liquid chromatography–mass spectrometry (LC–MS) at different time points (Supplementary Figure 1). NfsB-mCherry linearized the cyclic cMO in a dose- and time-dependent manner, with 4 nM enzyme completely cleaving the 4-NB linker within 1 h.

Having established the ability of NfsB to linearize 4-NB cyclic cMOs *in vitro*, we investigated the efficacy of this uncaging reaction in live organisms. *Ntla* is required for notochord and posterior mesoderm development, and both tissues are ablated in *ntla* mutants.^{20,21} Zebrafish lacking *ntla* function also exhibit somite defects due to the absence of notochord-derived signals. We therefore co-injected the 4-NB *ntla* cMO and varying amounts of *nfsB-mCherry* mRNA into zebrafish zygotes and observed the resulting phenotypes at 24 h post fertilization (hpf) (Figure 2a and b). Using a morphology-based scoring system for *ntla* loss-of-function phenotypes,^{1,22} we found that phenotypic strength correlated with *nfsB-mCherry* mRNA levels, plateauing at an embryonic dose of 400 pg. Nonspecific developmental defects were not observed with any experimental condition, indicating that 4-NB cMOs do not become cytotoxic upon NfsB-mediated activation. To better understand the relationship between *nfsB-mCherry* mRNA dose and enzyme concentration, we examined NfsB-mCherry protein levels in 5-hpf embryos by quantitative Western blot analysis with an anti-mCherry antibody (Supplementary Figure 2). Using purified mCherry protein as a standard, we estimated NfsB-mCherry levels to be 3 pg/embryo, which corresponds to an *in vivo* concentration of 1 nM.

To verify *Ntla* depletion in zebrafish embryos co-injected with the 4-NB *ntla* cMO and *nfsB-mCherry* mRNA, we analyzed

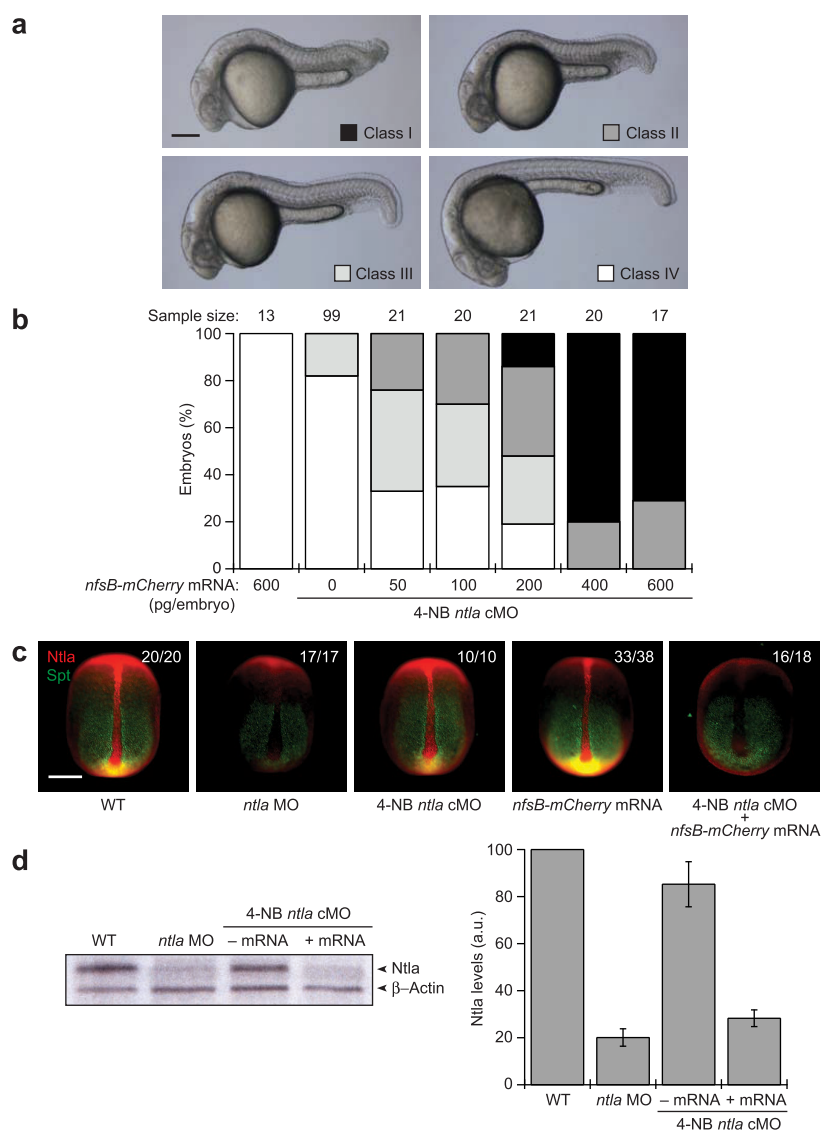


Figure 2. Enzymatic activation of 4-NB cyclic cMOs in *nfsB-mCherry* mRNA-injected zebrafish. (a) Classification of *ntla* loss-of-function phenotypes (I = most severe, IV = wildtype). 24-hpf embryos are shown (lateral view, anterior left). Scale bar: 200 μ m. (b) Phenotypic distributions for embryos injected with 4-NB *ntla* cMO (115 fmol/embryo) and varying amounts of *nfsB-mCherry* mRNA. (c) Immunostaining of Ntle protein in embryos injected with the 4-NB *ntla* cMO (115 fmol/embryo) and/or *nfsB-mCherry* mRNA (400 pg/embryo). Spadetail (Spt/Tbx16) protein within the paraxial mesoderm was also immunostained to confirm embryo orientations (since *spt* expression is regulated by Ntle,³² Spt protein levels are reduced upon Ntle knockdown). Representative 10-hpf embryos are shown (dorsal view, anterior up), and the penetrance of each phenotype is indicated. Scale bar: 200 μ m. (d) Western blot analysis of Ntle expression in 10-hpf embryos injected with indicated reagents. Reagent doses: *ntla* MO or cMO, 115 fmol/embryo; *nfsB-mCherry* mRNA, 400 pg/embryo. A representative blot and quantification of the Ntle levels normalized with respect to β -actin are shown. Graphical data are the average of three independent experiments \pm sem.

Ntle protein levels by whole-mount immunostaining. While embryos injected with either 4-NB *ntla* cMO or *nfsB-mCherry* mRNA alone exhibited wildtype-like Ntle expression, co-injection of the two reagents caused significant loss of Ntle protein (Figure 2c). Similar results were obtained by Western blot analyses of Ntle levels, with the 4-NB *ntla* cMO achieving a functional dynamic range approaching that of its light-activatable DMNB counterpart¹¹ (Figure 2d).

To conclude our studies, we evaluated the performance of NfsB-activatable cMOs in zebrafish that stably express the triggering enzyme in a tissue-specific manner. As in mammals, principal islet formation in zebrafish involves two waves of pancreatic endocrine cell differentiation.^{23–25} Dorsal bud-derived β cells begin to emerge at the 12-somite stage (15 hpf) and increase in number as somitogenesis continues;

ventral bud-derived progenitors contribute to a second phase of endocrine differentiation between 1 and 3 days post fertilization (dpf). The transcription factors *pancreatic and duodenal homeobox 1* (*pdx1*) and *motor neuron and pancreas homeobox 1* (*mnx1*) act cooperatively to promote β cell development,^{26,27} with *pdx1* expressed broadly throughout the developing pancreas and *mnx1* localized to the dorsal bud.^{24,28} Both factors become more restricted to the principal islet, and their expression is sustained as the cells differentiate into endocrine tissue. Accordingly, zebrafish embryos co-injected with conventional *pdx1* and *mnx1* MOs are completely devoid of these insulin-producing cells.²⁶

To specifically knockdown Pdx1 and Mnx1 in insulin-producing cells, we synthesized 4-NB cyclic cMOs targeting *pdx1* (10b, 5'-GATAGTAATGCTCTTCCCCGATTCAT-3')

and *mnx1* (10c, 5'-TTTTTAGATTTCTCCATCTGCCCA-3') and co-injected them into transgenic zebrafish expressing *nfsB* under control of the *insulin* promoter [*Tg(insulin:CFP-nfsB)*]. Wildtype zebrafish co-injected with the 4-NB *pdx1* and *mnx1* cMOs exhibited normal β cell differentiation, as visualized by *insulin* expression in 3-dpf larvae (Figure 3).

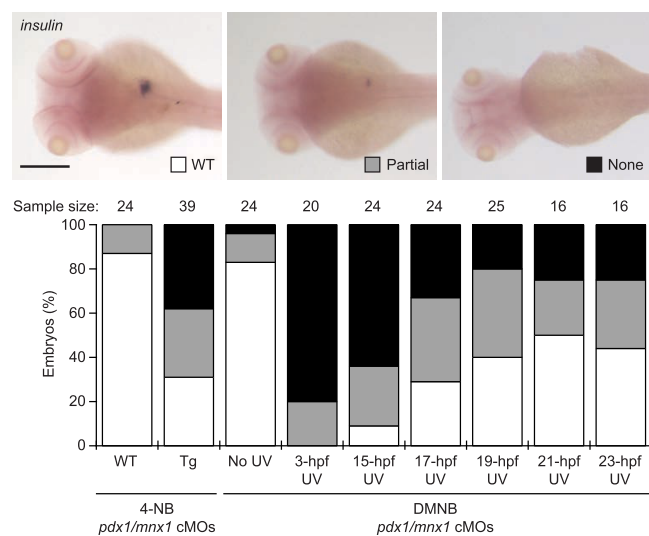


Figure 3. Enzymatic activation of 4-NB cyclic cMOs in transgenic zebrafish. (a) Classification of endocrine pancreas phenotypes as gauged by *insulin*-expressing cells. 3-dpf larvae are shown (dorsal view, anterior left). Scale bar: 200 μ m. (b) Phenotypic distributions for wildtype larvae injected with NfsB-activatable 4-NB cMOs or homozygous *Tg(insulin:CFP-nfsB)* larvae injected with either 4-NB cMOs or light-activatable DMNB cMOs. cMOs targeting *pdx1* or *mnx1* were used in combination (250 fmol/embryo each), and all injections were conducted at the one- to four-cell stage. Embryos injected with the DMNB cMOs were irradiated with 360 nm light at the indicated time points.

However, the NfsB-activatable reagents significantly inhibited endocrine differentiation in *Tg(insulin:CFP-nfsB)* larvae, with approximately 70% exhibiting a partial or complete loss of *insulin*-producing cells. Our results indicate that *pdx1* and *mnx1* are required after the initiation of *insulin* transcription to maintain β cell fates and that their cell-autonomous function accounts for most of this activity, even though both factors are more broadly expressed.

We next compared these phenotypes with those obtained with light-activatable DMNB cMOs. We co-injected wildtype zebrafish with DMNB cMOs targeting *pdx1* and *mnx1* and irradiated them with 360 nm light at various developmental stages. Photoactivation of the DMNB cMOs at 17 hpf disrupted principal islet formation to a similar extent as the NfsB-activatable cMOs, whereas earlier irradiation times led the ablation of nearly all β cells (Figure 3). These observations suggest that 4-NB cMO activation occurs within the first 2–3 h of *insulin* promoter-dependent *nfsB* transcription, consistent with the *in vitro* kinetics we observed with nanomolar enzyme concentrations.

Taken together, our findings validate the concept of enzyme-activatable cMOs and establish NfsB as an effective uncaging reagent. The use of NfsB as the triggering enzyme is particularly attractive, since transgenic organisms that express this bacterial nitroreductase are continually being engineered for cell ablation studies. 4-NB cMOs will significantly expand the versatility of

these NfsB-expressing lines, as they will enable gene knock-downs in the targeted tissues. Multiple genes could be rapidly interrogated through this experimental strategy, and a broad spectrum of cell types could be accessed through known *cis* regulatory elements. The discovery of NfsB mutants with greater catalytic activity promises to enhance the effectiveness of this approach,²⁹ and we anticipate that the development of additional enzyme/cMO pairs could enable orthogonal, combinatorial gene silencing in model organisms.

METHODS

Reagents. Reagents and procedures used to synthesize cMOs are provided in Supporting Information. T2KXIG Δ IN-derived *insulin:nfsB-mCherry* vector¹⁸ was provided by M. Parsons. mCherry protein and rabbit anti-mCherry polyclonal antibody were purchased from BioVision, mouse anti-Spt monoclonal antibody from the Zebrafish International Resource Center, mouse anti- β -actin antibody from Sigma, and rabbit anti-Ntla polyclonal antibody was previously generated by our laboratory.¹³ HEK-293T cells were purchased from the American Type Culture Collection.

In Vitro Characterization of 4-NB cMO Activation. The T2KXIG Δ IN-derived *insulin:nfsB-mCherry* vector was digested with XhoI/NotI, and the excised fragment was cloned into similarly cut pCS2+ plasmid, placing *nfsB-mCherry* downstream of the CMV promoter. To obtain NfsB-mCherry protein, HEK-293T cells were cultured in DMEM containing 10% fetal bovine serum, 100 U/mL penicillin, 0.1 mg/mL streptomycin, and 1 mM L-glutamine. After the cells reached 60% confluency, they were transfected with the pCS2+ *nfsB-mCherry* vector using TransIT-LT1 reagent (Mirus Bio), cultured for 3 days, and then lysed with 25 mM Tris-HCl, pH 7.4 buffer containing 150 mM NaCl, 1 mM EDTA, 1% (v/v) NP-40%, and 5% (v/v) glycerol.

NfsB-mCherry protein was purified from the cell lysates using immobilized rabbit anti-mCherry polyclonal antibody. Ten micrograms of the antibody was mixed with 20 μ L Protein A/G Plus Agarose (Pierce) in 10 mM sodium phosphate, pH 7.2 buffer containing 150 mM NaCl for 60 min at RT. After washing the resin with the same buffer, the antibody was cross-linked to the beads with disuccinimidyl suberate for another 60 min. NfsB-mCherry was bound to the antibody-cross-linked resin in cell lysis buffer for 2 h at 4 $^{\circ}$ C, and the resin was then washed with fresh lysis buffer and equilibrated with Tris-buffered saline (TBS). The fusion protein was then eluted with 4 M MgCl₂, exchanged into 1X PBS through dialysis (2-kDa MWCO Slide-A-Lyzer, Pierce), and quantified by Western blot using purified mCherry protein as a standard.

The ability of NfsB to linearize the 4-NB *ntla* cMO was then assessed by combining the cyclic oligonucleotide (0.2 nmol), NADH (10 nmol), and varying amounts of NfsB-mCherry protein in 100 μ L 1X PBS. Each mixture was incubated at 28.5 $^{\circ}$ C for 1–4 h, at which point the reaction was stopped by the addition of 400 μ L ice-cold methanol and diluted with an equal volume of water. The samples were then lyophilized, dissolved in 10 μ L water, and analyzed by LC-MS.

Zebrafish Aquaculture and Husbandry. All zebrafish (*Danio rerio*) procedures were performed on embryos obtained from wildtype AB (Zebrafish International Resource Center) or *Tg(insulin:CFP-nfsB)*¹⁹ (provided by R. Anderson) zebrafish, in compliance with protocol 10511 approved by the Institutional Animal Care and Use Committee of the Stanford University School of Medicine. Embryos used in these studies were obtained by natural matings and cultured in E3 embryo medium at 28.5 $^{\circ}$ C. Homozygous *Tg(insulin:CFP-nfsB)* embryos were used for 4-NB cMO experiments.

Oligonucleotide Injections. MO and cMO solutions containing 100 mM KCl and 0.1% (w/v) phenol red were prepared, and each solution was heated to 100 $^{\circ}$ C for 30 s to dissociate MO aggregates. The MO/cMO solution was microinjected to one- to four-cell stage zebrafish (2 nL/embryo). 5'-capped *nfsB-mCherry* mRNA was generated from SacII-linearized pCS2+ *nfsB-mCherry* using an

mMESSAGE mMACHINE SP6 kit (Ambion). The resulting transcripts were solubilized in water containing 100 mM KCl and 0.1% (w/v) phenol red and mixed with the cMO solution as necessary. Zebrafish zygotes were microinjected with the mRNA-containing solutions (2 nL/embryo). All injections were conducted in E3 medium, and the embryos were subsequently cultured in this medium at 28.5 °C.

Whole-Mount Immunostaining and *in Situ* Hybridization. To detect Ntla and Spt proteins in bud-stage (10 hpf) zebrafish, the embryos were fixed with 4% (w/v) paraformaldehyde in 1X PBS overnight at 4 °C. The embryos were then immunostained with rabbit anti-Ntla polyclonal antibody (1:500 dilution), mouse anti-Spt monoclonal antibody (1:100 dilution), Alexa Fluor 594-conjugated anti-rabbit IgG (H+L) antibody (1:200 dilution), and Alexa Fluor 488-conjugated anti-mouse IgG (H+L) antibody (1:200 dilution) as previously described.⁷ To detect *insulin* transcripts in 3-dpf zebrafish, the larvae were fixed with 4% (w/v) paraformaldehyde in 1X PBS for 1 h at RT. Whole-mount *in situ* hybridization was then performed,³⁰ using an *insulin* antisense riboprobe labeled with digoxigenin.³¹ To generate the *insulin* riboprobe, RNA was isolated from wildtype 3-dpf zebrafish embryos using an RNeasy Plus kit (Qiagen) and then converted to cDNA using the SuperScript III First-Strand Synthesis System (Invitrogen). The primers 5'-CCATATCCACCATTCTCG-CC-3' and 5'-TAATACGACTCACTATAGGCAAACGGAGAGCA-TTAAGGCC-3' were then used to amplify the full-length *proproinsulin* gene and add a T7 promoter. The resulting PCR product was purified with a QIAquick PCR purification kit (Qiagen), and digoxigenin-labeled RNA was prepared from this template using a MEGAscript T7 Transcription kit (Invitrogen).

Western Blot Analysis of Zebrafish Embryos. Wildtype and cMO-injected embryos were manually deyolked in TM1 buffer (1% (w/v) PEG-200,000, 100 mM NaCl, 5 mM KCl, and 5 mM HEPES pH 7.0) at the 5-hpf stage (for immunoblotting with anti-Cherry antibody) or bud stage (for immunoblotting with anti-Ntla antibody). Twenty deyolked embryos from each experimental condition were then homogenized in SDS-PAGE loading buffer (50 μ L/sample; 330 mM 2-mercaptoethanol, 100 mM DTT, 4% (w/v) glycerol, and 100 mM Tris-HCl, pH 6.8), vortexed, and heated to 100 °C for 5 min. The resulting lysates were electrophoretically resolved on a 4–12% acrylamide gradient gel (10 μ L/lane) and blotted onto nitrocellulose. The membrane was incubated with blocking solution (0.2% (w/v) I-Block, 0.1% (v/v) Tween 20, and 1X PBS) and probed with anti-Ntla antibody (1:100 dilution) or anti-mCherry antibody (1:1,000 dilution) or anti- β actin antibody (1:2,000 dilution). Chemiluminescence detection was then conducted using a goat anti-rabbit IgG (H+L) horseradish peroxidase conjugate (Invitrogen; 1:10,000 dilution in 1X PBS containing 0.1% (v/v) Tween 20) and SuperSignal West Dura substrate (Pierce), and protein band intensities were quantified using a ChemiDoc XRS system and ImageQuant software (Bio-Rad).

Photoactivation of DMNB cMOs. Zebrafish embryos were arrayed in an agarose template (560 μ m \times 960 μ m wells), with the animal pole facing the light source. To irradiate DMNB cMO-injected embryos, mercury lamp light was focused onto individual embryos for 10 s (3-hpf embryos) or 15 s (15-, 17-, 19-, 21-, and 23-hpf embryos) using a Leica DM4500B compound microscope equipped with an HCX APO 20 \times /0.5 NA water-immersion objective and A4 filter cube (Ex: 360 nm, 40 nm bandpass). The optimum irradiation conditions were determined previously using caged fluorescein dextran.¹¹ For photoactivation of cMOs in 3-hpf *Tg(insulin:CFP-nfsB)* zebrafish, the entire embryo was irradiated with 360 nm light. At later developmental time points, the region of 360 nm illumination was positioned to encompass the CFP-positive pancreatic field.

Zebrafish Imaging. To permit live imaging of zebrafish at 24 h post fertilization (hpf), the embryos were manually dechorionated and immobilized in E3 medium containing 0.2% (w/v) low-melt agarose and 0.05% (w/v) tricaine mesylate. For imaging of fixed zebrafish, the embryos and larvae were mounted in 100% glycerol. Brightfield images were acquired using a Leica M205FA stereoscope equipped with a Leica DFC500 digital camera. Fluorescence images were obtained with

a Leica DM4500B compound microscope equipped with GFP and Texas Red filter sets and a Retiga-SRV digital camera.

■ ASSOCIATED CONTENT

● Supporting Information

Supplementary figures, synthetic procedures, and NMR spectra. This material is available free of charge via the Internet at <http://pubs.acs.org>.

■ AUTHOR INFORMATION

Corresponding Author

*E-mail: jameschen@stanford.edu.

Notes

The authors declare no competing financial interest.

■ ACKNOWLEDGMENTS

We thank M. Parsons for the *insulin:nfsB-mCherry* plasmid, R. Anderson for *Tg(insulin:CFP-nfsB)* zebrafish, and E. Hyde, A. Payumo, and E. Ober for helpful discussions. This work was supported by the NIH (R01 GM087292, DP1 HD075622, and P50 GM107615 to J.K.C.), a Japan Society for the Promotion of Science Fellowship (S.Y.), and an A. P. Giannini Foundation Fellowship for Medical Research (L.E.M.).

■ REFERENCES

- (1) Shestopalov, I. A., and Chen, J. K. (2010) Oligonucleotide-based tools for studying zebrafish development. *Zebrafish* 7, 31–40.
- (2) Summerton, J., and Weller, D. (1997) Morpholino antisense oligomers: design, preparation, and properties. *Antisense Nucleic Acid Drug Dev.* 7, 187–195.
- (3) Heasman, J., Kofron, M., and Wylie, C. (2000) Beta-catenin signaling activity dissected in the early *Xenopus* embryo: a novel antisense approach. *Dev. Biol.* 222, 124–134.
- (4) Nasevicius, A., and Ekker, S. C. (2000) Effective targeted gene 'knockdown' in zebrafish. *Nat. Genet.* 26, 216–220.
- (5) Kos, R., Reedy, M. V., Johnson, R. L., and Erickson, C. A. (2001) The winged-helix transcription factor FoxD3 is important for establishing the neural crest lineage and repressing melanogenesis in avian embryos. *Development* 128, 1467–1479.
- (6) Howard, E. W., Newman, L. A., Oleksyn, D. W., Angerer, R. C., and Angerer, L. M. (2001) SpKrl: a direct target of beta-catenin regulation required for endoderm differentiation in sea urchin embryos. *Development* 128, 365–375.
- (7) Shestopalov, I. A., Sinha, S., and Chen, J. K. (2007) Light-controlled gene silencing in zebrafish embryos. *Nat. Chem. Biol.* 3, 650–651.
- (8) Tomasini, A. J., Schuler, A. D., Zebala, J. A., and Mayer, A. N. (2009) PhotoMorphs: a novel light-activated reagent for controlling gene expression in zebrafish. *Genesis* 47, 736–743.
- (9) Tallafuss, A., Gibson, D., Morcos, P., Li, Y., Seredick, S., Eisen, J., and Washbourne, P. (2012) Turning gene function ON and OFF using sense and antisense photo-morpholinos in zebrafish. *Development* 139, 1691–1699.
- (10) Deiters, A., Garner, R. A., Lusic, H., Govan, J. M., Dush, M., Nascone-Yoder, N. M., and Yoder, J. A. (2010) Photocaged morpholino oligomers for the light-regulation of gene function in zebrafish and *Xenopus* embryos. *J. Am. Chem. Soc.* 132, 15644–15650.
- (11) Yamazoe, S., Shestopalov, I. A., Provost, E., Leach, S. D., and Chen, J. K. (2012) Cyclic caged morpholinos: conformationally gated probes of embryonic gene function. *Angew. Chem., Int. Ed.* 51, 6908–6911.
- (12) Wang, Y., Wu, L., Wang, P., Lv, C., Yang, Z., and Tang, X. (2012) Manipulation of gene expression in zebrafish using caged circular morpholino oligomers. *Nucleic Acids Res.* 40, 11155–11162.

- (13) Shestopalov, I. A., Pitt, C. L., and Chen, J. K. (2012) Spatiotemporal resolution of the Ntla transcriptome in axial mesoderm development. *Nat. Chem. Biol.* 8, 270–276.
- (14) Moore, J. C., Sheppard-Tindell, S., Shestopalov, I. A., Yamazoe, S., Chen, J. K., and Lawson, N. D. (2013) Post-transcriptional mechanisms contribute to Etv2 repression during vascular development. *Dev. Biol.* 384, 128–140.
- (15) Zenno, S., Koike, H., Tanokura, M., and Saigo, K. (1996) Gene cloning, purification, and characterization of NfsB, a minor oxygen-insensitive nitroreductase from *Escherichia coli*, similar in biochemical properties to FRase I, the major flavin reductase in *Vibrio fischeri*. *J. Biochem.* 120, 736–744.
- (16) Clark, A. J., Iwobi, M., Cui, W., Crompton, M., Harold, G., Hobbs, S., Kamalati, T., Knox, R., Neil, C., Yull, F., and Gusterson, B. (1997) Selective cell ablation in transgenic mice expression *E. coli* nitroreductase. *Gene Ther.* 4, 101–110.
- (17) Kwak, S. P., Malberg, J. E., Howland, D. S., Cheng, K. Y., Su, J., She, Y., Fennell, M., and Ghavami, A. (2007) Ablation of central nervous system progenitor cells in transgenic rats using bacterial nitroreductase system. *J. Neurosci. Res.* 85, 1183–1193.
- (18) Pisharath, H., Rhee, J. M., Swanson, M. A., Leach, S. D., and Parsons, M. J. (2007) Targeted ablation of beta cells in the embryonic zebrafish pancreas using *E. coli* nitroreductase. *Mech. Dev.* 124, 218–229.
- (19) Curado, S., Anderson, R. M., Jungblut, B., Mumm, J., Schroeter, E., and Stainier, D. Y. (2007) Conditional targeted cell ablation in zebrafish: a new tool for regeneration studies. *Dev. Dyn.* 236, 1025–1035.
- (20) Halpern, M. E., Ho, R. K., Walker, C., and Kimmel, C. B. (1993) Induction of muscle pioneers and floor plate is distinguished by the zebrafish no tail mutation. *Cell* 75, 99–111.
- (21) Schulte-Merker, S., van Eeden, F. J., Halpern, M. E., Kimmel, C. B., and Nusslein-Volhard, C. (1994) no tail (ntl) is the zebrafish homologue of the mouse T (Brachyury) gene. *Development* 120, 1009–1015.
- (22) Ouyang, X., Shestopalov, I. A., Sinha, S., Zheng, G., Pitt, C. L., Li, W. H., Olson, A. J., and Chen, J. K. (2009) Versatile synthesis and rational design of caged morpholinos. *J. Am. Chem. Soc.* 131, 13255–13269.
- (23) Biemar, F., Argenton, F., Schmidtke, R., Epperlein, S., Peers, B., and Driever, W. (2001) Pancreas development in zebrafish: early dispersed appearance of endocrine hormone expressing cells and their convergence to form the definitive islet. *Dev. Biol.* 230, 189–203.
- (24) Field, H. A., Dong, P. D., Beis, D., and Stainier, D. Y. (2003) Formation of the digestive system in zebrafish. II. Pancreas morphogenesis. *Dev. Biol.* 261, 197–208.
- (25) Hesselson, D., Anderson, R. M., Beinat, M., and Stainier, D. Y. (2009) Distinct populations of quiescent and proliferative pancreatic beta-cells identified by HOTcre mediated labeling. *Proc. Natl. Acad. Sci. U.S.A.* 106, 14896–14901.
- (26) Kimmel, R. A., Onder, L., Wilfinger, A., Ellertsdottir, E., and Meyer, D. (2011) Requirement for Pdx1 in specification of latent endocrine progenitors in zebrafish. *BMC Biol.* 9, 75.
- (27) Dalgin, G., Ward, A. B., Hao, T., Beattie, C. E., Nechiporuk, A., and Prince, V. E. (2011) Zebrafish *mnx1* controls cell fate choice in the developing endocrine pancreas. *Development* 138, 4597–4608.
- (28) Wendik, B., Maier, E., and Meyer, D. (2004) Zebrafish *mnx* genes in endocrine and exocrine pancreas formation. *Dev. Biol.* 268, 372–383.
- (29) Mathias, J. R., Zhang, Z., Saxena, M. T., and Mumm, J. S. (2014) Enhanced cell-specific ablation in zebrafish using a triple mutant of *Escherichia coli* nitroreductase. *Zebrafish* 11, 85–97.
- (30) Thisse, C., and Thisse, B. (2008) High-resolution in situ hybridization to whole-mount zebrafish embryos. *Nat. Protoc.* 3, 59–69.
- (31) Milewski, W. M., Duguay, S. J., Chan, S. J., and Steiner, D. F. (1998) Conservation of PDX-1 structure, function, and expression in zebrafish. *Endocrinology* 139, 1440–1449.
- (32) Griffin, K. J., and Kimelman, D. (2003) Interplay between FGF, one-eyed pinhead, and T-box transcription factors during zebrafish posterior development. *Dev. Biol.* 264, 456–466.